SCIENCE CHINA
Information Sciences

• RESEARCH PAPER • doi: 10.1007/s11432-015-5421-8

Adaptive controller design for underwater snake robot with unmatched uncertainties

Anfan ZHANG[1,3], Shugen MA[1,2], Bin LI[1], Minghui WANG[1]*, Xian GUO[1] & Yuechao WANG[1]

[1] *State Key Laboratory of Robotics, Shenyang Institute of Automation, Chinese Academy of Sciences, Shenyang* 110016*, China;*
[2] *Department of Robotics, Ritsumeikan University, Shiga-ken* 525-8577*, Japan;*
[3] *University of Chinese Academy of Sciences, Beijing* 100049*, China*

Received June 17, 2015; accepted August 21, 2015

Abstract Because of hydrodynamic model error of the present dynamic model, there is a challenge in controller design for the underwater snake-like robot. To tackle this challenge, this paper proposes an adaptive control schemes based on dynamic model for a planar, underwater snake-like robot with model error and time-varying noise. The adaptive control schemes aim to achieve the adaptive control of joint angles tracking and the direction of locomotion control. First, through approximation and reducibility using Taylor expansion method, a simplified dynamics model of a planar amphibious snake-like robot is derived. Then, the L1 adaptive controller based on piecewise constant adaptive law is applied on the simplified planar, underwater snake-like robot, which can deal with both matched and unmatched nonlinear uncertainties. Finally, to control the direction of locomotion, an auxiliary bias signal is used as the control input to regulate the locomotion direction. Simulation results show that this L1 adaptive controller is valid to deal with different uncertainties and achieve the joint angles tracking and fast adaptive at the same time. The modified L1 adaptive controller, in which the auxiliary bias item is added, has the ability to change the direction of locomotion, that is, the orientation angle is periodic with arbitrarily given constant on average.

Keywords underwater snake-like robot, adaptive control, simplified system, piecewise constant law, unmatched uncertainties, underactuated robots

Citation Zhang A F, Ma S G, Li B, et al. Adaptive controller design for underwater snake robot with unmatched uncertainties. Sci China Inf Sci, 2016, 59, doi: 10.1007/s11432-015-5421-8

1 Introduction

Snake-like robots have a strong environment adaptiveness, so researchers have shown great interest to snake-like robot in the last few decades. They make every effort to develop snake robot physical mechanisms [1], model, and controller for snake locomotion. Underwater snake-like robot, which is made for moving in unknown water, has many degrees of freedom and is more complicated than conventional mobile robots in the dependence on environment interaction. In recent years, many underwater snake-like robot models are proposed [2–6]. These models are complex, highly coupled and not efficient enough.

* Corresponding author (email: mhwang@sia.cn)

The difference between different dynamics models for the underwater snake-like robot is hydrodynamic modeling. The liquid characteristic changes very fast under different Reynolds number. Resistance model is suitable for low Reynolds number [7], Lighthill reaction model based on the theory of slender is suitable for high Reynolds number [8], and the improved model based on Jordan method is suitable for medium Reynolds number [9]. Therein, only the significant hydrodynamic effects were included in all the above models, in which the less-significant unmodeled hydrodynamics is neglected. Generally speaking, time-varying of the hydrodynamics coefficient is also not considered in those literatures. Those reasons cause model error and uncertainties. The full nonlinear dynamic equation, underactuated characteristic and uncertainties result in some difficulties in the controller design. One of the challenges in underwater snake-like robot with those uncertainties (matched and unmatched) is adaptive controller design.

Currently, the adaptive control has already been researched in robot area [10–16]. Adaptive control based on the reference model of underwater snake-like robot has not been investigated in the literature yet. The major challenges of adaptive control are the high-coupling dynamic equation, many degrees of freedom and underactuated characteristic. One possible approach would be normal Model Reference Adaptive Control (MRAC) [17], which is composed of reference system, feedback controller, adaptive estimator, and plant. This method needs to satisfy the condition that the reference system is time-invariant. However, it cannot deal with unknown time-varying nonlinearities. Another feasible approach is a modified MRAC scheme where the basic architecture is based on the internal model principle, named L1 adaptive controller [18]. It can deal with unknown time-varying nonlinearities and guarantee higher robustness. L1 adaptive controller, whose adaptation rate can be directly associated with the sampling rate of the available CPU [19], is a fast estimation scheme and ensures uniform transient response in addition to steady-state tracking. L1 adaptive controller has been applied on NASA Air STAR Flight Test Vehicle. Others such as gain scheduling method can cope with the unavoidable nonlinearities and time-varying dynamics of the practical plant and are compensating for known static nonlinearities [20]. The main disadvantage of gain scheduling is that it is an open loop adaptation scheme, without real learning taking place. Sliding-mode control approach for systems with mismatched uncertainties via a nonlinear disturbance observer [21] is also an available choice.

In this paper, we consider adaptive controller design of the planar, underwater snake-like robot in medium Reynolds number. Firstly, the Newton-Euler method is used to derive the full nonlinear model. Instead of controller design for a full nonlinear dynamical model of snake-like robot system, we will first simplify the model through Taylor series and describe function. The skills of simplification are described for the purpose of analytical studies and controller design. Then, the L1 adaptive controller is adopted to track the joint angles. We apply the L1 adaptive control based on a piecewise constant adaptive law on the system of the simplified snake-like robot. The main reasons are as follows: (1) the controller can be implemented for planar amphibious snake-like robot systems, adjustment or tuning procedure, (2) the controller is robust to unmodeled dynamics (mainly induced by two-order drag force form) and parametric model uncertainties (neglect limited items and high-order items of Taylor series) and hydrodynamic coefficient time-varying property, (3) L1 adaptive controller shows better performance in the given hardware (CPU and sensor) condition compared with the PD controller or less requirement for computation for a given performance. Finally, in order to achieve the locomotion direction control, an auxiliary input is used as control input to stabilize the average orientation. This is the first time that L1 adaptive control based on a piecewise constant adaptive law is applied on underwater snake-like robot. This adaptive control design method may be viewed as a direction of future actual control of snake-like robot which also meets the requirement of current research.

The structure of this paper is as follows. In Section 2, we briefly introduce the third generation of our snake-like robot and give the hydrodynamic model of our underwater snake-like robot, and also provide an approximate dynamic model. Section 3 introduces L1 adaptive controller design procedure and the adaptive controller modification by adding an auxiliary bias to the L1 adaptive controller to control the orientation. Section 4 gives simulation results and demonstrates the performance of L1 adaptive control system of the underwater snake-like robot to illustrate the effectiveness of the modified adaptive controller. Finally, Section 5 presents some concluding remarks.

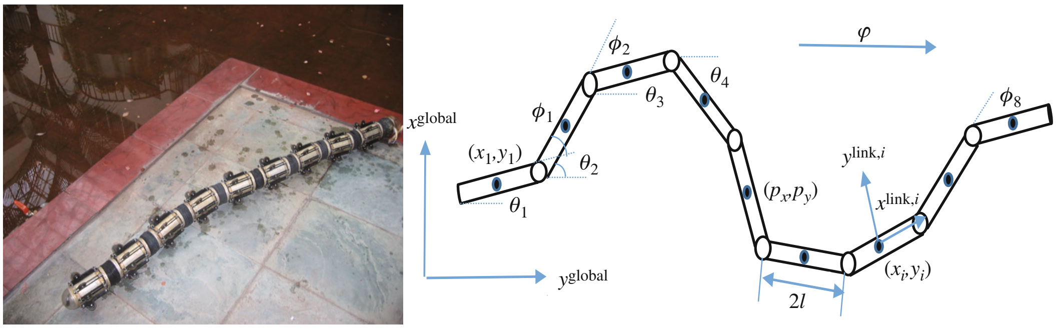

Figure 1 (Color online) The prototype of underwater snake-like robot and its kinematic parameters.

Table 1 Scale parameters of the amphibious snake-like robot

Total weight (kg)	Total length (m)	Diameter of the trunk (m)	Single modules length (m)
6.75	1.17	0.075	0.125

2 Simplified model

Underwater snake-like robot and land snake-like robot move in the water and on the land separately. Because amphibious snake-like robot can move both in the water and on the land, amphibious snake-like robot can be used to research the underwater locomotion mechanism. Firstly, our amphibious planar snake-like robot prototype is presented before modeling, which is waterproof and can move smoothly both in the water and on the land and mainly is composed of nine modular universal units. The details can be found in [22, 23]. The scale parameters of the amphibious snake-like robot are listed in Table 1. The parameters of the prototype will be used in the hydrodynamics coefficient calculation and simulation. The following is the hydrodynamic model.

2.1 Hydrodynamic modeling

It is worthy and necessary to mention the hydrodynamic modeling because of its complication. Although Navier-Stokes equations can be a good description of force acting on the liquid dynamic balance, it is time-consuming to solve the Navier-Stokes equation. Besides, due to coupling and high nonlinearity and infinite dimensional state of the surrounding fluid, analytic hydrodynamic modeling is necessary for the convenience of design of the controller. Three most widely used analytical models of hydrodynamics are proposed by Taylor [7], Lighthill [8] and Morison [24], respectively. Taylor's model is suitable for low Reynolds numbers, and Lighthill'model is appropriate for high Reynolds number and slender body. Marison's model is suitable for moderate Reynolds number. Most of the literature did not consider the current and fluid moment. Fluid torque is taken into account but implemented in an numerical integration method [5, 6]. A solution to this issue was proposed by Kelasidi [4, 25], whose method not only considers the moment of hydrodynamic force, but also the current and nonlinear viscous drag. His model is adapted here to suit our needs, and then, let nonlinear drag and moment form act as unmodeled dynamic to make the simulation as close as possible to the real one.

We will present the hydrodynamics model of the planar snake-like robot consisting of n links of length $2l$ interconnected by $n-1$ active joints. Reynolds number for our snake locomotion is about 10^4–10^5, which is moderate Reynolds number. Assume that the robot is a slender body with a cylindrical trunk. This approach takes into account both the linear drag forces (resistive fluid forces), the added mass effect (reactive fluid forces) and the fluid moments. The nonlinear drag forces and nonlinear torque items are taken into account as unmodeled dynamics uncertainties. The planar snake-like robot is identical with mass m, moment of inertia $\frac{1}{3}ml^2$, orientation angle φ, vector $\phi = [\phi_1, \phi_2, \ldots, \phi_{n-1}]^{\mathrm{T}} \in \mathbb{R}^{n-1}$, and absolute angles in global frame $\theta = [\theta_1, \ldots, \theta_n]^{\mathrm{T}}$. The prototype of underwater snake-like robot and the kinematic parameters of the snake robot are defined in terms of the symbols depicted in Figure 1. Snake robot moves in the horizontal plane. The fluid forces exerted on link i in i body frame are expressed on the mass center of the link i as

$$f_{r,i}^{\text{link},i} = \begin{bmatrix} c_t & 0 \\ 0 & c_n \end{bmatrix} \times v_{r,i}^{\text{link},i} + \begin{bmatrix} c_t & 0 \\ 0 & c_n \end{bmatrix} \times |v_{r,i}^{\text{link},i}| v_{r,i}^{\text{link},i} + \begin{bmatrix} 0 & 0 \\ 0 & u_n \end{bmatrix} \times \dot{v}_{r,i}^{\text{link},i},$$

where $c_t = \pi\rho C_f R l$, $u_n = \pi\rho C_a R^2 l$, and $c_n = 2\pi\rho C_D R l$, $v_{r,i}^{\text{link},i}$ is center of mass velocity in i body frame. Because of underwater snake-like robots' slender body shape, in the x-direction, form drag is omitted and only viscous resistance is to be considered, while in the y-direction, we ignored the viscous resistance and only considered the form drag. Besides, we ignored the added mass force in x-direction.

The torque applied on link i by the fluid is modeled in the following form:

$$\tau_i = -\lambda_1 \ddot{\theta}_i - \lambda_2 \dot{\theta}_i - \lambda_3 |\dot{\theta}_i| \dot{\theta}_i.$$

For a cylinder, the added mass torque reduces to a simple form with the parameter λ_1 expressed as [4,25]

$$\lambda_1 = \frac{1}{3} l^2 \times C_M \times m_{\text{added}},$$

where C_M is the added inertia coefficient. Additionally, we derive the parameters λ_2 and λ_3 by integrating the drag torque. The drag force on a $2l$ length of link i due to link rotation produces a drag torque on the CM of the link, which is given by

$$\tau_{\text{drag},i} = -\int_{-l}^{l} (s C_{\text{Ldx}} s\dot{\theta}_i + s C_{\text{Ldx}} \text{sgn}(s\dot{\theta}_i)(s\dot{\theta}_i)^2) \mathrm{d}s = -\lambda_2 \dot{\theta}_i - \lambda_3 \dot{\theta}_i |\dot{\theta}_i|,$$

where λ_2 and λ_3 are given by $\lambda_2 = \frac{2}{3}\pi\rho C_D R l^4$ and $\lambda_3 = \frac{1}{2}\pi\rho C_D R l^4$. The cross section is of circular shape, so the drag torque coefficient induced by the normal drag force per unit length is given by $C_{\text{Ldx}} = \frac{1}{2}\rho\pi R C_D$.

2.2 The simplified underwater snake-like robot model

We choose the Newton-Euler method to model the underwater snake-like robot and start with the full nonlinear equations of motion derived in the literature [25, 26], which already avoid a singularity issue in this model presented in [4] by redefining the expression of link accelerations. The reason is that it may be used for amphibious snake robots moving both on land and in water, and the force and torque balance equations are in matrix form, which means that it will be easy for simplification. The torque balance equations and force balance equations for all links are expressed in the form

$$J_0 \ddot{\theta} + [l S_\theta K, -l C_\theta K] \begin{bmatrix} m\ddot{X} - f_x \\ m\ddot{Y} - f_y \end{bmatrix} - \tau = D^{\mathrm{T}} u, \quad \begin{bmatrix} \ddot{p_x} \\ \ddot{p_y} \end{bmatrix} = \frac{1}{nm} E^{\mathrm{T}} \begin{bmatrix} f_x \\ f_y \end{bmatrix},$$

where $f_x \in \mathbb{R}^n$ is the fluid force acting on all links in body x-direction and $f_y \in \mathbb{R}^n$ is the fluid force acting on all links in body y-direction. The joint torques on all links in vector form are $u(t) \in \mathbb{R}^{n-1}$. The fluid moments in vector form are τ. p_x and p_y are the global coordinates of the center of mass of the robot. n is the number of the links. For other terms, please refer to Appendix A. Generally, most of the model can be rewritten in this form $\dot{x} = f(x, u)$. However, it is difficult to rewrite the above model. The original equations are too complicated, fully nonlinear and highly coupled. It is hard to design the controller and gain insights into the locomotion mechanisms, which are the reasons why this paper simplified the underwater snake-like robot equation.

We adopt Taylor series expansion to reduce the coefficients of the model. That is to say, we use the main item to approximate the nonlinear equation. This paper treats the truncation of higher order terms and other remainders as unmodeled dynamics and treats white noise as disturbance. Assuming that ϕ, φ, $\dot{p}_x$, and ω are small, and choosing a reference velocity in x-direction $\dot{p}_{x0}$, the definitions for the coefficients and details are given in Appendix A. To this end, the underwater snake-like model is reduced to

$$\ddot{\phi} + \mu\dot{\phi} + M_{v1}(\dot{p}_{x0})\phi + \sigma_\phi = J_1^{-1}u, \tag{1}$$

$$\ddot{\varphi} + \mu\dot{\varphi} + M_{v2}(\dot{p}_{x0})\phi + \sigma_\varphi = -J_2^{-1}J_{21} \times J_{11}^{-1}u, \tag{2}$$

$$\begin{bmatrix} \ddot{p_x} \\ \ddot{p_y} \end{bmatrix} = \frac{1}{nm}E^{\mathrm{T}} \begin{bmatrix} f_x \\ f_y \end{bmatrix}. \tag{3}$$

Eq. (1) describes the relationship of the joint torques $u(t) \in \mathbb{R}^{n-1}$ and joint angles. Eq. (2) shows how the joint torques indirectly control the orientation angle φ. Eq. (3) shows that the locomotion velocity is directly controlled by the shape change ϕ, only the amplitudes of ϕ and φ are small enough, the model qualitatively captures the essential dynamics of snake-like robot locomotion and is reasonably accurate for the range of undulations observed in animals [27]. Accordingly, the full nonlinear dynamics equation can be reduced to approximate dynamics equations. In this paper, we keep the center mass velocity equation in the nonlinear equation item, which means the force equation is not simplified.

There inevitably exist the uncertainty and unmodeled dynamics due to the truncation and reduction of snake-like robot model and as a result of the transformation from coupling hydrodynamic model to the analytical and closed-form model. However, we can enclose the effect of the disturbances with L1 adaptive controller.

3 Adaptive controller design

3.1 L1 adaptive controller design

The objective of this paper is to find an adaptive controller which can handle the uncertainty and accomplish the joint control, such that the closed-loop system achieves three properties:

• The simplified snake-like robot system achieves joint angles steady-state tracking and ensures uniform transient response, and the steady-state error remains a small value.

• The adaptive controller compensates uncertainties caused by the time-varying parameters and unmodeled dynamics under the condition where the model is not accurate because of the reduction of the mathematical model.

• The system has the capability to control the snake-like robot movement orientation or make φ periodic with zero (constant value) average.

It is well known that the researchers have proved that any asymptotically stabilizable control law for a snake robot to an equilibrium point must be time-varying [28]. This conclusion implies the feasibility of L1 adaptive law method. Asymptotically stabilizing control law based on piecewise constant law for amphibious snake robots to an equilibrium point must be time-varying. Also, the controller is robust to unmodeled dynamics. Thus, we use the L1 adaptive law to deal with the simplified underwater snake-like robot MIMO system with nonlinear unmatched uncertainties. By introducing the state variables $x(t) = [\phi^{\mathrm{T}}, \dot{\phi}^{\mathrm{T}}]^{\mathrm{T}}$ and initial constant CM velocity in global x-direction $\dot{p}_{x0}$ (assuming 0.2 m/s), we can rewrite the above simplified model of the underwater snake-like robot equation (1) compactly in state space form as

$$\dot{x} = A_p x(t) + b\overline{u} + \sigma(t), \quad y(t) = c^{\mathrm{T}}x(t),$$

with

$$A_p = \begin{bmatrix} 0_{n-1,n-1} & I_{n-1,n-1} \\ -M_{v1}(\dot{p}_{x0}) & -\mu I_{n-1,n-1} \end{bmatrix}, \quad b = \begin{bmatrix} 0_{n-1,n-1} \\ J_1^{-1} \end{bmatrix}, \quad c^{\mathrm{T}} = \begin{bmatrix} I_{n-1,n-1} \\ 0_{n-1,n-1} \end{bmatrix}^{\mathrm{T}}.$$

$\sigma(t) = \begin{bmatrix} 0_{n-1,n-1} \\ -\sigma_\phi \end{bmatrix}$ + noise is the output and the state vector of internal unmodeled dynamics, and vector noise contains time-varying noise or random noise. The system state vector $x(t) = [\phi, \dot{\phi}]^{\mathrm{T}}$ is measured for feedback. $\overline{u}(t)$ are the control input signals. $y(t) = \phi(t) \in \mathbb{R}^{n-1}$ are the outputs of joint angles.

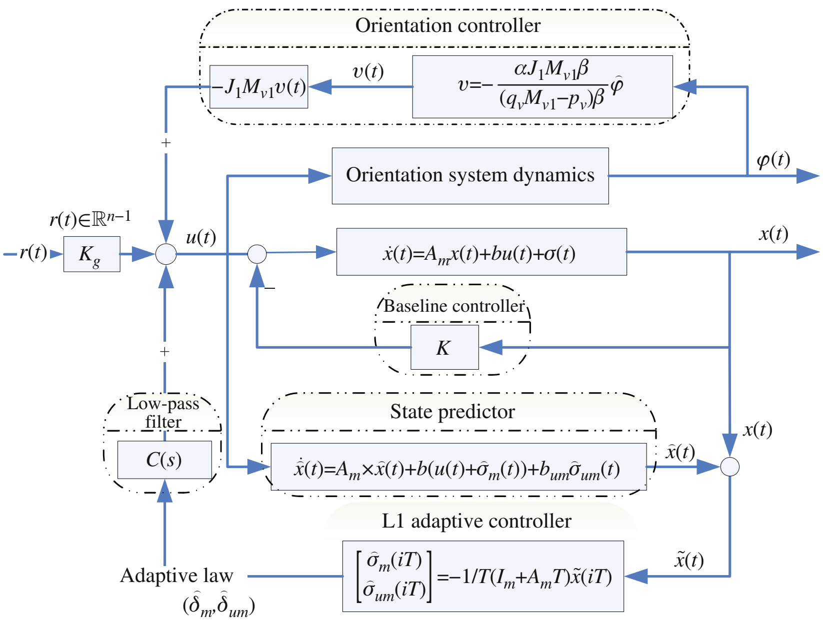

Figure 2 (Color online) The modified adaptive controller structure.

However, A_p is not Hurwitz (does not satisfy the condition of piecewise constant control law). We use pole-placement method to get a new closed-loop system (even though the actual system's pole is variational, such volatility fluctuates around a constant value). Next, we design state feedback controller without changing the zero point of single input and single output system. Let $\overline{u}(t) = -Kx(t) + u(t)$, where K is state feedback gain matrix, and u presents the external inputs, then we get new state feedback closed-loop system with nonlinear unmatched uncertainties:

$$\dot{x} = A_m x(t) + bu(t) + \sigma(t), \quad y(t) = c^{\mathrm{T}} x(t), \quad x(0) = x0,$$

where $A_m = A_p - b \times K$, $\sigma(t) \in \mathbb{R}^{2n-2}$ is unknown nonlinear function vector. A_m is a known $(2n-2) \times (2n-2)$ Hurwitz matrix, $b \in \mathbb{R}^{(2n-2)\times(n-1)}$ is a known constant matrix, (A_m, b) is controllable, and c^{T} is a known full-rank constant matrix, (A_m, c^{T}) is observable. The system can be rewritten by the form

$$\dot{x} = A_m x(t) + bu(t) + b\sigma_m + b_{um}\sigma_{um}, \quad y(t) = c^{\mathrm{T}} x(t), \quad x(0) = x0, \tag{4}$$

where $b_{um} \in \mathbb{R}^{(2n-2)\times(n-1)}$ is a constant matrix such that $b^{\mathrm{T}} \times b_{um} = 0$, $\mathrm{rank}(b, b_{um}) = 2n-2$, and $\sigma_m(t) \in \mathbb{R}^{n-1}$, $\sigma_{um}(t) \in \mathbb{R}^{n-1}$ is unknown nonlinear function vector meeting the requirements that $[\sigma_m(t),\ \sigma_{um}(t)] = B^{-1}\sigma_1(t)$, where $B = [b, b_{um}]$. The L1 adaptive controller is extensively described in reference [29]. This paper adopts L1 adaptive controller based on piecewise constant adaptive law, see details in [18]. In this section, we present the process of the L1 adaptive controller design based on piecewise constant adaptive law. The whole closed-loop control system of this paper is illustrated in Figure 2.

State-predictor: considering the following state predictor here

$$\dot{\hat{x}}(t) = A_m\hat{x}(t) + bu(t) + b\hat{\sigma}_m(t) + b_{um}\hat{\sigma}_{um}(t), \quad y(t) = c^{\mathrm{T}}\hat{x}(t), \quad \hat{x}(0) = x0.$$

The perturbance is decomposed into b_{um} and b direction, and L1 adaptive controller can compensate disturbance on the b_{um} direction (unmatched uncertainties). The purpose of using state predictor is to estimate the derivative of the system states, so as to achieve rapid adaptive.

Adaptive laws: the piecewise constant adaptive laws based on Euler one fixed step size are as follows:

$$\begin{bmatrix}\hat{\sigma}_m(iT)\\ \hat{\sigma}_{um}(iT)\end{bmatrix} = -\frac{1}{T}(I_{2n-2} + A_m T)\tilde{x}(iT),$$

where $\tilde{x}(iT)=\hat{x}(iT)-x(iT)$ is the prediction error, and the adaptive controller uses fixed step size T Euler 1 method. In this model, parameters $\sigma_m,\ \sigma_{um}$ are replaced by $\hat{\sigma}_m,\ \hat{\sigma}_{um}$ respectively.

Control law: the controller signal u(t) is generated in the frequency domain by

$$u(s)=K_g r(s)-C_1(s)\hat{\sigma}_m(s)-C_2(s)H_m^{-1}(s)H_{um}(s)\hat{\sigma}_{um}(s),$$

where $H_m=c^{\mathrm{T}}(s\times I_{2n-2}-A_m)^{-1}b,\ H_{um}=c^{\mathrm{T}}(s\times I_{2n-2}-A_m)^{-1}b_{um},\ r(s)\in\mathbb{R}^{n-1}$ are the reference signals, while the prefilter $K_g(s)$ is chosen as the constant matrix $K_g=-(c^{\mathrm{T}}(A_m)^{-1}b)^{-1}$ to achieve decoupling among the signals. Second-order filter is chosen as the low-pass filter $C_1(s),\ C_2(s)$, which will be given in Section 4. The high-frequency components of ϕ will be suppressed by the low-pass filter, while the remaining will be the actual control input. However, the L1 adaptive controller can only finish the first two goals.

3.2 L1 adaptive controller modification

The third control objective is to control the snake-like robot locomotion direction or make orientation angle φ periodic with zero (constant value) average, which cannot be achieved by the above L1 adaptive controller. We know that

$$\vartheta_i=A_{\mathrm{ref}}\sin(\omega t+(i-1)\beta_{\mathrm{ref}})+\gamma.$$

Given γ nonzero constant, we can realize a circular path. The direction of turn (left or right) is determined by the sign of γ. The greater γ is, the bigger curvature is. The direction of locomotion can be steered by joint angles [26]. We adopt an auxiliary bias signal $\nu(t)\in\mathbb{R}$ to stabilize the orientation dynamics. The adaptive adjustment of ϕ with error $\beta\nu$ gives ν directly proportional to φ. Refs. [27, 30] used this method to regulate the orientation and also explained the principle of the method. We will show why the auxiliary input $\nu(t)$ can be used to stabilize locomotion direction. Assume φ_0 is constant such that $\bar{\varphi}(t)\to\varphi_0$. We choose the control input u so that

$$\phi=\vartheta+\beta\nu, \tag{5}$$

where $\vartheta=[\vartheta_1,\ldots,\vartheta_i,\ldots,\vartheta_{n-1}]$ and ϑ_i is the expected (reference) joint angle of link i. Firstly, we define the "error" signal ξ by

$$\xi:=q_v^{\mathrm{T}}(\phi-\vartheta)-(\varphi-\varphi_0), \tag{6}$$

where $q_v^{\mathrm{T}}:=-J_2^{-1}J_{21}\times J_{11}^{-1}\times J_1$. Then, eliminating joint torque from (1) and (2) and substituting (5), we have

$$\ddot{\xi}+\mu\dot{\xi}+b^{\mathrm{T}}\beta\nu+h=0,\quad b:=M_{v1}(\dot{p}_{x0})^{\mathrm{T}}q_v-p_v^{\mathrm{T}},\quad h=q^{\mathrm{T}}(\ddot{\vartheta}+\mu\dot{\vartheta})+b^{\mathrm{T}}\vartheta,$$

where $p_v=M_{v2}(\dot{p}_{x0})$. We set $\nu=\kappa(s)\xi$ with linear dynamics $\kappa(s)$ to meet the condition that the transfer function from h to ξ is stable. In this paper, the average value of $q^{\mathrm{T}}\sigma_\phi-\sigma_\varphi$ is 0. Then by lemma (details in [30]): the linear and stable system has the character that the average value of the output converges to zeros whenever the input average does so. Since $\bar{h}(t)\to 0$ due to $\bar{\vartheta}(t)\to 0$, then $\bar{\xi}\to 0$. Also, $\kappa(s)$ is stable, then we have $\bar{\varphi}-\varphi_0\to 0$. Thus, we can regulate the orientation by choosing the feedback control u, which satisfies the condition that $\phi=\vartheta+\beta\nu$ with a stable $\kappa(s)$ satisfying the transfer function stable condition $s^2+\mu s+b^{\mathrm{T}}\beta\kappa(s)=0\Rightarrow\mathrm{Root}(s)<0$. We eliminate ξ from $\nu=\kappa(s)\xi$ and get

$$\nu=\frac{\kappa(s)}{\kappa(s)q_v^{\mathrm{T}}\beta-1}(\varphi-\varphi_0).$$

We will show how to choose u to make the system hold steady state. The signal $\phi-\beta\nu$ converges to ϑ, and we rewrite (1) as

$$(\ddot{\phi}-\beta\ddot{\nu})+\mu(\dot{\phi}+\beta\dot{\nu})+M_{v1}(\dot{p}_{x0})\times(\phi-\beta\nu)=J_1^{-1}u-\beta(\ddot{\nu}+\mu\dot{\nu})-M_{v1}(\dot{p}_{x0})\beta\nu. \tag{7}$$

The control input u_{new} is given by

$$u_{\mathrm{new}}=u+J_1(\beta(\ddot{\nu}+\mu\dot{\nu})+M_{v1}(\dot{p}_{x0})\beta\nu), \tag{8}$$

where u_{new} is the control input of (7) and u is the control input of (1). If the signals $\nu,\ \dot{\nu}$ change very slowly, then $\dot{\nu} \approx 0,\ \ddot{\nu} \approx 0$. We have approximately

$$u_{\text{new}} = u + J_1 \times (M_{v1}(\dot{p}_{x0})\beta\nu). \tag{9}$$

In order to achieve this goal, we introduce dynamics equation about ν in [30], where ν is generated from φ through the following dynamics:

$$q_v^{\mathrm{T}}\beta(\ddot{\nu} + \mu \times \dot{\nu}) + b^{\mathrm{T}}\beta\nu + \eta_1 \times (\hat{\varphi} - \varphi_0) = 0, \quad (\hat{\varphi} - \varphi_0) + \eta_2\dot{\hat{\varphi}} = (\varphi - \varphi_0),$$

where $\mu^2 \geqslant \eta_1 \geqslant 0,\ \beta \in \mathbb{R}^{n-1}$ is a constant vector [30]. We have approximately

$$\nu(t) = -\frac{\eta_1}{(q_v^{\mathrm{T}} M_{v1}(\dot{p}_{x0}) - M_{v2}(\dot{p}_{x0}))\beta}(\varphi - \varphi_0). \tag{10}$$

Ultimately, the controller is

$$u_{\text{new}}(s) = K_g r(s) + J_1 \times M_{v1}(\dot{p}_{x0})\beta\nu(s) - C_1(s)\hat{\sigma}_1(s) - C_2(s)H_m^{-1}(s)H_{um}(s)\hat{\sigma}_2(s), \tag{11}$$

where $C_2(s)H_m^{-1}(s)H_{um}(s)\hat{\sigma}_2(s)$ compensates the mismatched uncertainties, and $C_1(s)\hat{\sigma}_1(s)$ eliminates the matched uncertainties and smooth control signals. $K_g r(s)$ is used to produce the expected joint angles item. $J_1 \times M_{v1}(\dot{p}_{x0})\beta\nu(s)$ regulates the motion direction by adjusting each joint angle. Using this controller, we can achieve the goal of steady-state tracking of joint angles (approximate natural oscillation) and let the average orientation converge to the expected value. Of course, the response of the system will be fast. This controller can effectively eliminate the uncertainties and maintain smooth control signals.

4 Simulation results and discussion

4.1 Simulation results

This section shows the simulation results of underwater snake-like robot and demonstrates performance of the proposed controller. In this paper, we consider the underwater snake-like robot with links $n = 9$, single modular length $2l = 0.125$, mass $m = 6.75/9$, and radius $R = 0.075/2$, which is identical with the physical robot presented in Section 2. We focus on serpentine locomotion, where the joint angle is given by

$$\vartheta_i = A_{\text{ref}} \sin(\omega t + (i-1)\beta_{\text{ref}}) + \gamma.$$

In order to make the closed-loop system stable, we choose the closed systems poles using pole place method. The pole value must be larger than ω. Because if we choose lower poles values, the reference signals will be suppressed by the system. By choosing desired and reasonable closed-loop poles, we obtain the feedback gain matrix K. The related hydrodynamic coefficients are as follows [4–6, 25]: $C_f = 0.03, C_D = 1, C_a = 1, C_M = 1$, the normal drag coefficient for the environmental force is set to $c_n = 9.3750$, and the tangential drag coefficient is set to $c_t = 0.2209$, and the added mass coefficients are set to $u_n = 0.5522, u_t = 0$. Choosing $\dot{p}_{x0} = 0.2$ m/s as the reference velocity in x-direction, we get the desired closed-loop system. The sampling time is $T = 0.01$ s, and two-order filter is set to

$$C(s) = \frac{75}{(s+5)(s+15)}.$$

The vector $\beta = e, e := [1, \ldots, 1]$, the closed-loop system is then simulated with arbitrarily initial condition, and parameters are selected as $\phi(0) = \text{zeros}(n-1),\ \varphi(0) = 0$. The remaining states are 0.

For the first time, the L1 adaptive controller is applied onto the snake-like robot model. The performance of the L1 adaptive controller (not the modified adaptive controller) is investigated in a tracking problem. Firstly, we consider the ideal controller signal for the system in (4) in frequency domain as

$$u_{\text{id}}(s) = -(\delta_m(s) + H_m^{-1}(s)H_{um}(s)\delta_{um}(s) - K_g(s)r(s)), \tag{12}$$

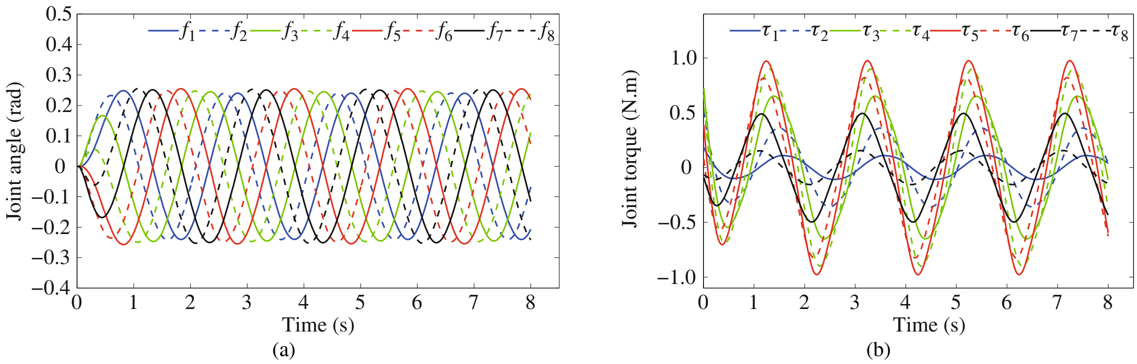

Figure 3 L1 adaptive controller for serpentine locomotion: all joint with unmodeled dynamics. (a) Snake-like robot joint angles; (b) snake-like robot joint torques.

which means the uncertainties can be full compensated by $u_{\rm id}$, and the desired system output response in frequency domain is

$$y_{\rm id} = H_m(s)K_g(s)r(s).$$

In practical application, there are more or less various kinds of noise because of change in the environment and the characteristics of the snake-like robot system itself, such as unmodeled dynamics from model error, random disturbance from system of the input, sensor measurement noise, high-frequency disturbances from high-order items of Taylor series and flow disturbance and so on. In order to illustrate the L1 adaptive controller has the ability to deal with model error and various kinds of noise, simulation results about tracking error between $y(t)$ and $y_{\rm id}$ as well as $u(t)$ and $u_{\rm id}$ under three different disturbances will be presented for the same tracking purposes: $A_{\rm ref} = \pi/10, \omega = \pi, \beta_{\rm ref} = \pi/4, \gamma = 0$. Case 1: White noise and unmodeled dynamics as disturbance, noise $=$ rand$(2n-2,1)$. Case 2: Constant noise mix with high-frequency sinusoidal disturbance and unmodeled dynamics as disturbance, noise $= [\text{zeros}(n-1,1); \text{ones}(n-1,1) \times \sin(5\pi t + \frac{\pi}{4} + \text{ones}(n-1,1) \times 3.7]$. Case 3: Only unmodeled dynamics as disturbance, noise $=$ zeros$(2n-2,1)$. We employ three cases to verify the performance of L1 adaptive controller, use white noise to simulate the random disturbance, and use high-frequency sinusoidal disturbance to simulate high-frequency disturbances. Subscript bar stands for actual system, and subscript 2 stands for joint 2.

All joint output signals and all control input of snake-like robot with unmodeled dynamics are shown in Figure 3 (a) and (b), respectively. We only give the joint 2 simulation results for concise illustration, and other joint angle inputs have the similar characteristics. Figure 4(a) shows the second joint angle output signal. The difference between the actual joint angle and the desired joint angle output (uncertainties are full compensated) is not obvious, which means the performance of the joint tracking is good; the corresponding control input is also shown in Figure 4(b). This figure illustrates that the control input signal is almost the same as the expected control input. Controller has the capability to compensate the white noise and deals with model error, but would lead to the jitter problem of the control torque input. Figure 5 (a) and (b) show the second joint angle output and the control input of the snake-like system with disturbance which contains constant and high-frequency sinusoidal. This figure shows that L1 controller can near-complete compensate this type of disturbance.

The output (the second joint angle) signal and the control torque input signal (the second joint angle) are shown in Figure 6 (a) and (b), respectively. In this case, only the nonlinear unmodeled dynamics is to be considered. Comparing Figure 6 with the other two figures, the actual output joint angle and the expected output joint angle are almost overlapping on each case in the presence of different disturbances, and the tracking error between $\phi(t)$ and $\vartheta(t)$ as well as $u(t)$ and $u_{\rm ideal}(t)$ can achieve arbitrary closeness by reducing T. The input signals can track the reference signals and compensate for the different uncertainties (admissible). We can see that the L1 architecture achieves the fast estimation. It is worth mentioning that only Case 1 contains nonzero unmatched uncertainties. So, Figure 4(a) shows

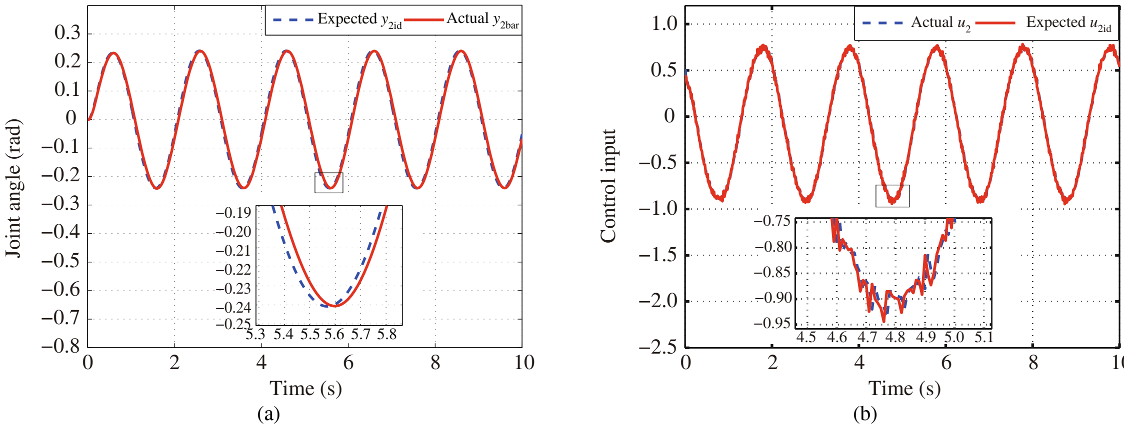

Figure 4 (Color online) L1 adaptive controller for serpentine locomotion: joint 2 with white noise. (a) Profile of joint angle of joint 2 with white noise; (b) profile of control input of joint 2 with white noise.

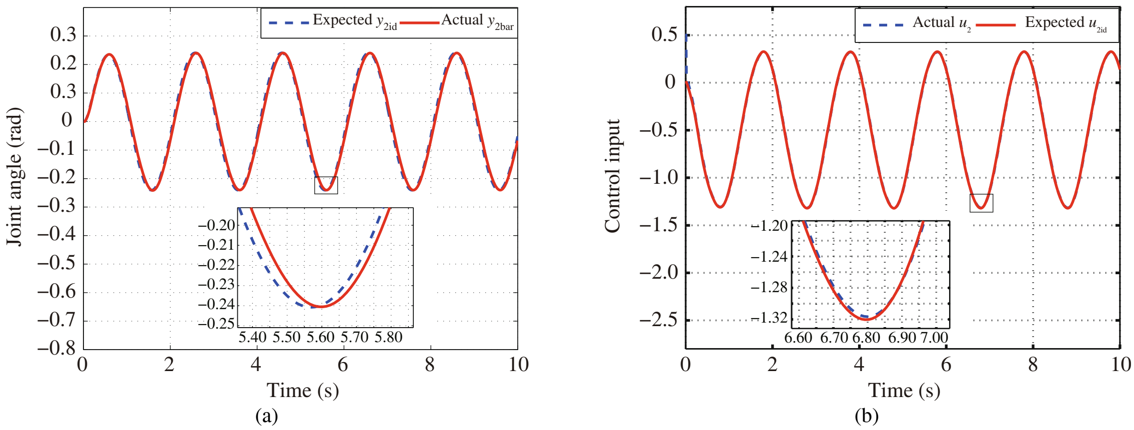

Figure 5 (Color online) L1 adaptive controller for serpentine locomotion: joint 2 with constant noise mix with high-frequency sinusoidal disturbance. (a) Profile of joint angle of joint 2 with constant noise mix with high-frequency sinusoidal disturbance; (b) profile of control input of joint 2 with constant noise mix with high-frequency sinusoidal disturbance.

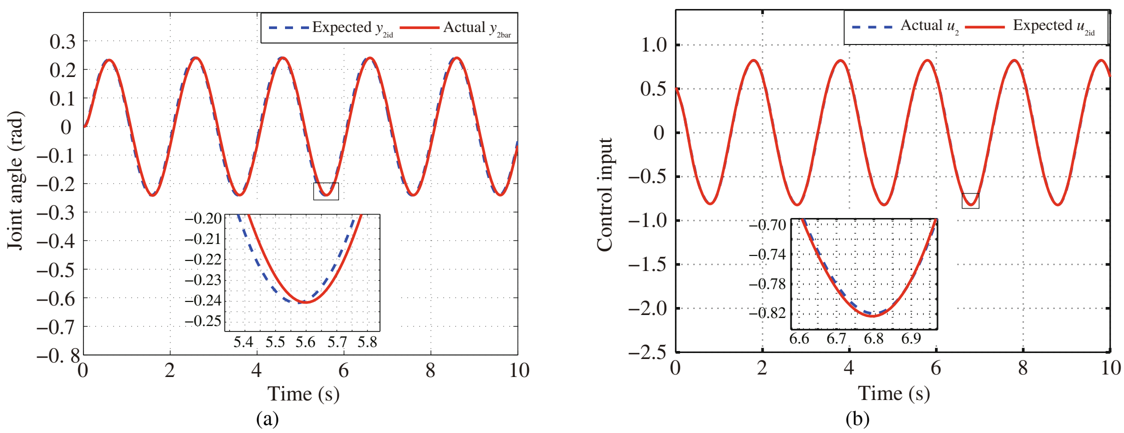

Figure 6 (Color online) L1 adaptive controller for serpentine locomotion: joint 2 with unmodeled dynamics. (a) Profile of joint angle of joint 2 with unmodeled dynamics; (b) profile of control input of joint 2 with unmodeled dynamics.

that L1 adaptive controller can deal with unmatched uncertainties (induced by white noise). Without auxiliary bias being added in the adaptive controller, locomotion direction is uncontrolled. While with auxiliary signals, the orientation gives constant φ_0 regardless of the initial state.

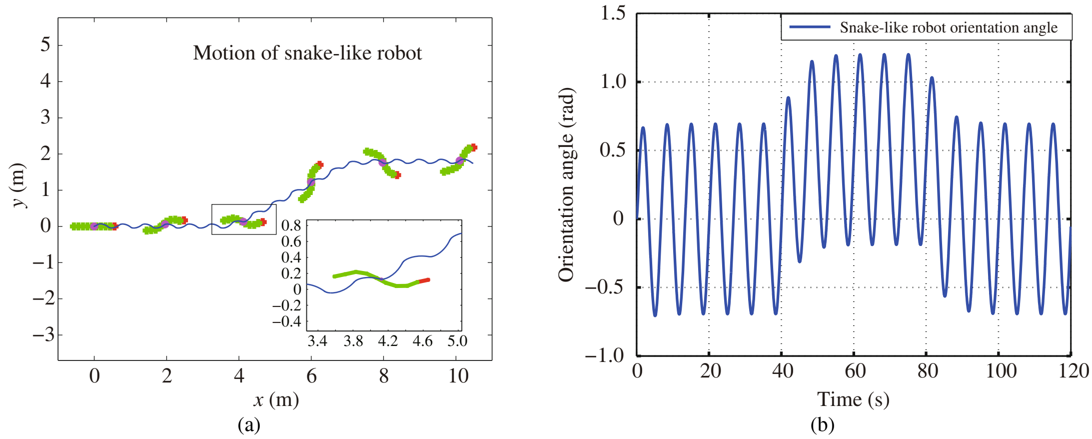

Figure 7 (Color online) The modified adaptive controller for serpentine locomotion: the change in the position and orientation. (a) The blue line represents center of mass trajectory of snake-like robot and the green line represents the instantaneous motion of snake robot per 23 s (the red line stands for the head of snake-like robot); (b) the change in the orientation angle φ of snake-like robot. 0 s $\leqslant$ Time $<$ 40 s, $\varphi_0 = 0$, 40 s $\leqslant$ Time $<$ 80 s, $\varphi_0 = \frac{\pi}{6}$, Time $\geqslant$ 80 s, $\varphi_0 = 0$.

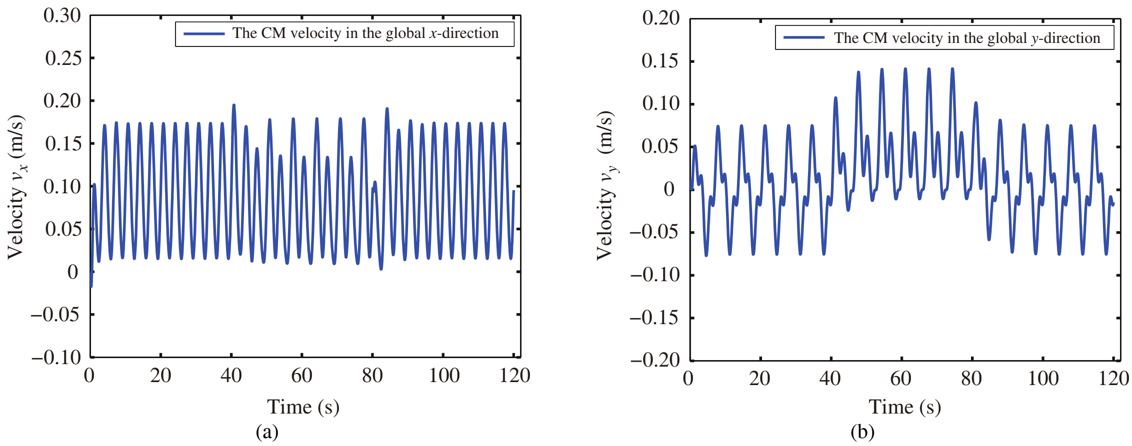

Figure 8 (Color online) The modified adaptive controller for serpentine locomotion: the CM velocity of snake-like robot in the global coordinates. (a) The CM velocity $\dot{p}_x$; (b) the CM velocity $\dot{p}_y$.

Next, in order to illustrate the validity of the modified adaptive controller, we set $\varphi_0 = 0$, $t <$ 40 s; $\varphi_0 = \frac{\pi}{6}$, 40 s $\leqslant t <$ 80 s; $\varphi_0 = 0$, $t \geqslant$ 80 s. The parameters of reference joint angles are selected as $A_{\rm ref} = \pi/8$, $\omega = 0.3\pi$, $\beta_{\rm ref} = \pi/4$, $\gamma = 0$. The orientation angle and the center mass motion are expressed in Figure 7. This figure also shows the motion of the snake. This figure shows that this method can steer the direction of locomotion. What is more, reducing the sampling time T can further reduce the steady-state error. Figure 8 (a) and (b) show the CM velocity of the snake robot in the global x-direction and y-direction, respectively. The average velocity in the x-direction is up to about 0.1 m/s. We can see that the system output is able to converge to the desired reference signal quickly even there exists a large initial tracking error. We can observe that the tracking performance under different disturbances is better. As a result, we can conclude that the controller's design is reasonable and available. However, the method tends to consume a relatively long time, and the dimension of state variable in the inverse system is large. Steady-state error is $\tilde{x}(t) = \sigma(t)T$, and transient and steady-state error can achieve arbitrarily close tracking (joint angle). The difference between the actual disturbances and the estimated disturbances is very small. This method cannot achieve zero steady-state error, but can be systematically improved by reducing sampling time. This filter may eliminate the noise signal if the frequency of the disturbance is known.

4.2 Discussion

To deal with hydrodynamics model error and uncertainties because of environmental interaction and model simplification, we introduced the adaptive controller. In order to gain the insights into locomotion mechanisms and control design, we simplified the nonlinear equation. Although the uncertainties will increase because of model simplification, the uncertainties can be transformed into linear time-varying problem that the L1 adaptive controller can deal with. The snake robot is multilink system, in which multiple degrees of freedom make them difficult to control. Normal MRAC integral controller obviously loses its phase margin and even causes high-frequency oscillation in the presence of fast adaptation. L1 adaptive controller can make up for it with low-pass filter. The simulation results in Figures 4–6 supported this viewpoint and also showed that control signals were smooth. This is because the low-pass filter eliminates the high-frequency signals caused by high gain feedback ($\frac{1}{T}$). Besides, tracking joint angle output signals is fast because of high gain feedback $\frac{1}{T}$. Compared with sliding-model control which is applied on an anguilliform robotic fish to deal with parameter uncertainties [31], the joint tracking performance of the modified adaptive control is better. Besides, the modified control scheme can steer the direction of locomotion.

So far, input-output linearization was commonly adopted to finish tracking control for snake robot joints [32], which has shortcoming with poor robustness. On the other hand, joint offset is used to control the direction of the motion, which makes a worse result of path following. Thus, the modified adaptive control schemes proposed in this paper, which integrate the advantages of L1 controller, can solve the above problems. The results of this paper show that the presented adaptive control scheme can provide high performance in terms of speed and accuracy in the presence of uncertainties. An integral LOS path following controller was proposed for an underwater snake robot [25], and the proposed path following controller contains the heading controller component

$$\gamma = K_{\varphi}(\overline{\varphi} - \overline{\varphi}_{\mathrm{ref}}),$$

where $K_{\varphi} > 0$ is a control gain and $\overline{\varphi}_{\mathrm{ref}}$ is the mean value of the reference orientational angle of the snake-like robot φ_{ref}. Compared with the modified adaptive controller, the heading control law belongs to P controller and $K_{\varphi} > 0$ cannot be chosen arbitrarily. Orientation control law in this paper is complicated than heading control law. Actually, if we choose $\kappa(s) = 1$, orientation control law is the same as heading control law.

5 Conclusion

In this paper, we have derived the full nonlinear dynamic equation for planar, underwater snake-like robot in medium Reynolds number by Newton-Euler modeling method. This paper simplified the nonlinear dynamics equations by Taylor expansion method to derive the approximate dynamics equation for the purpose of controller design. L1 adaptive controller based on piecewise constant law for the simplified planar snake system with unmatched uncertainties was therefore proposed to track the expected joint angle. Since the considered mechanical system is underactuated for lack of direct control over the position and orientation angle, the auxiliary bias signals were thus added in the adaptive control law to regulate the orientation. The L1 adaptive controller was applied to the simplified snake-like robot system for the first time. The simulation demonstrated that the actual joint angle can track the reference joint angles quickly and accurately even suffering different disturbances, and also proved that L1 adaptive controller is effective for the approximate model. Furthermore, performance bounds can be systematically improved by reducing the sampling time. Besides, this paper added an auxiliary signal to achieve the goal of controlling the direction of locomotion. The full nonlinear center of mass motion equation illustrated the fact that locomotion direction control is valid. In the future research, this adaptive control method will be applied on the underwater snake-like robot as an experimental verification of the modified adaptive controller.

Acknowledgements This work was supported by National Natural Science Foundation of China (Grant No. 61333016).

Conflict of interest The authors declare that they have no conflict of interest.

References

1 Crespi A, Badertscher A, Guignard A, et al. AmphiBot I: an amphibious snake-like robot. Robot Auton Syst, 2005, 50: 163–175

2 Liljeback P, Pettersen K Y, Stavdahl O, et al. A simplified model of planar snake robot locomotion. In: Proceedings of IEEE/RSJ International Conference on Intelligent Robots and Systems (IROS), Taipei, 2010. 2868–2875

3 Tanaka M, Matsuno F. Experimental study of redundant snake robot based on kinematic model. In: Proceedings of IEEE International Conference on Robotics and Automation, Roma, 2007. 2990–2995

4 Kelasidi E, Pettersen K Y, Gravdahl J T, et al. Modeling of underwater snake robots. In: Proceedings of IEEE International Conference on Robotics and Automation, Hong Kong, 2014. 4540–4547

5 Khalil W, Gallot G, Ibrahim O, et al. Dynamic modeling of a 3-D serial eel-like robot. In: Proceedings of IEEE International Conference on Robotics and Automation, Barcelona, 2005. 1270–1275

6 Khalil W, Gallot G, Boyer F. Dynamic modeling and simulation of a 3-D serial eel-like robot. IEEE Trans Syst Man Cybern Part C-Appl Rev, 2007, 37: 1259–1268

7 Taylor G. Analysis of the swimming of long and narrow animals. Proc Roy Soc London Ser A, 1952, 214: 158–183

8 Lighthill M J. Large-amplitude elongated-body theory of fish locomotion. Proc Roy Soc London Ser B, 1971, 179: 125–138

9 Wiens J A. Gait optimization for a multilink anguilliform swimmer. Dissertation for the Doctoral Degree. Montreal: McGill University, 2012

10 He W, Ge S S, How B V E, et al. Robust adaptive boundary control of a flexible marine riser with vessel dynamics. Automatica, 2011, 47: 722–732

11 He W, Ge S S, Zhang S. Adaptive boundary control of a flexible marine installation system. Automatica, 2011, 47: 2728–2734

12 He W, Ge S S. Robust adaptive boundary control of a vibrating string under unknown time-varying disturbance. IEEE Trans Control Syst Technol, 2012, 20: 48–58

13 He W, Ge S S, Li Y, et al. Neural network control of a rehabilitation robot by state and output feedback. J Intell Robot Syst, 2015, 80: 15–31

14 Li Z, Ge S S, Ming A. Adaptive robust motion/force control of holonomic-constrained nonholonomic mobile manipulators. IEEE Trans Syst Man Cybern Part B-Cybern, 2007, 37: 607–616

15 Li Z, Li J, Kang Y. Adaptive robust coordinated control of multiple mobile manipulators interacting with rigid environments. Automatica, 2010, 46: 2028–2034

16 He W, Chen Y, Yin Z. Adaptive neural network control of an uncertain robot with full-State constraints. IEEE Trans Cybern, 2015, PP: 1–10

17 Narendra K S, Valavani L S. Direct and indirect model reference adaptive control. Automatica, 1979, 15: 653–664

18 Hovakimyan N, Cao C, Kharisov E, et al. Adaptive control for safety-critical systems. IEEE Control Syst, 2011, 31: 54–104

19 Hovakimyan N, Cao C. L1 Adaptive Control Theory. Philadelphia: Society for Industrial and Applied Mathematics, 2010

20 Lawrence D A, Rugh W J. Gain scheduling dynamic linear controllers for a nonlinear plant. Automatica, 1995, 31: 381–390

21 Utkin V I. Sliding Modes in Control and Optimization. Berlin: Springer-Verlag, 1992

22 Yu S, Ma S, Li B, et al. An amphibious snake-like robot with terrestrial and aquatic gaits. In: Proceedings of IEEE International Conference on Robotics and Automation, 2011. 2960–2961

23 Wang Y, Li B, Chen L, et al. Design and realization of snake-like robot control system. Robot, 2003, 6: 002

24 Morison J R, Johnson J W, Schaaf S A. The force exerted by surface waves on piles. J Petrol Technol, 1950, 2: 149–154

25 Kelasidi E, Pettersen K Y, Gravdahl J T. A waypoint guidance strategy for underwater snake robots. In: Proceedings of 22nd Mediterranean Conference of Control and Automation, Shanghai, 2014. 1512–1519

26 Saito. M, Fukaya M, Iwasakiost T. Serpentine locomotion with robotic snakes. IEEE Control Syst Mag, 2002, 22: 64–81

27 Blair J, Iwasaki T. Optimal gaits for mechanical rectifier systems. IEEE Trans Automat Contr, 2011, 56: 59–71

28 Liljeback P, Pettersen K Y, Stavdahl O, et al. Controllability and stability analysis of planar snake robot locomotion. IEEE Trans Automat Contr, 2011, 56: 1365–1380

29 Xargay E, Hovakimyan N, Cao C. L1 adaptive controller for multi-input multi-output systems in the presence of nonlinear unmatched uncertainties. In: Proceedings of American Control Conference, Baltimore, 2010. 874–879

30 Zhu L, Chen Z, Iwasaki T. Oscillation, orientation, and locomotion of underactuated multilink mechanical systems. IEEE Trans Control Syst Technol, 2013, 21: 1537–1548

31 Niu X. Modeling, control and locomotion planning of an anguilliform fish robot. Dissertation for the Doctoral Degree. Harbin: Harbin Institute of Technology, 2013. 26–76

32 Transeth A A, van De Wouw N, Pavlov A, et al. Tracking control for snake robot joints. In: Proceedings of IEEE/RSJ International Conference on Intelligent Robots and Systems, San Diego, 2007. 3539–3546

Appendix A The simplified model

We start with the fully nonlinear equations of motion derived in the literature [26] and [25], which already avoid a singularity issue of this model presented in [4] by redefining the expression of link accelerations, and we will show how to approximate and simplify the nonlinear equation. The torque balance equations and force balance equations for all links are expressed in the form as

$$J_0\ddot{\theta} + [lS_\theta K, -lC_\theta K]\begin{bmatrix} m\ddot{X} - f_x \\ m\ddot{Y} - f_y \end{bmatrix} - \tau = D^{\mathrm{T}}u, \quad \begin{bmatrix} \ddot{p_x} \\ \ddot{p_y} \end{bmatrix} = \frac{1}{nm}E^{\mathrm{T}}\begin{bmatrix} f_x \\ f_y \end{bmatrix},$$

with

$$\begin{bmatrix} m\ddot{X} - f_x \\ m\ddot{Y} - f_y \end{bmatrix} = \begin{bmatrix} m + u_n S_\theta^2 & -u_n S_\theta C_\theta \\ -u_n S_\theta C_\theta & m + u_n C_\theta^2 \end{bmatrix}\begin{bmatrix} \ddot{X} \\ \ddot{Y} \end{bmatrix} + \begin{bmatrix} c_t C_\theta^2 + c_n \times S_\theta^2 & (c_t - c_n)S_\theta C_\theta \\ (c_t - c_n)S_\theta C_\theta & c_t S_\theta^2 + c_n \times C_\theta^2 \end{bmatrix}\begin{bmatrix} \dot{X} \\ \dot{Y} \end{bmatrix} + \begin{bmatrix} c_t C_\theta & -c_n S_\theta \\ c_t S_\theta & c_n C_\theta \end{bmatrix}\begin{bmatrix} v_{rx}^2 \\ v_{ry}^2 \end{bmatrix}\operatorname{sign}\left(\begin{bmatrix} v_{rx} \\ v_{ry} \end{bmatrix}\right),$$

where $\theta \in \mathbb{R}^n$, $[X, Y]' \in \mathbb{R}^{2\times n}$, and J_0 is moment of inertia of all links written in matrix form. $[X, Y]'$ are global coordinates of the center of mass of all links written in matrix form. The torque applied on each link by the fluid can be modeled by

$$\tau = -\lambda_1\ddot{\theta} - \lambda_2\dot{\theta} - \lambda_3|\dot{\theta}|\dot{\theta},$$

where $\lambda_1 = \frac{l^2}{3}C_M m_a, \lambda_2 = \frac{2}{3}l^2 \times c_n$, and $\lambda_3 = \frac{1}{2}l^4 \times c_n$. In this paper, the added-mass coefficient of cylinder in y-direction is $m_a = \rho\pi R^2 \times 2l, C_M = 1$, so λ_1 can be rewritten in this form: $\lambda_1 = \frac{l^2}{3} \times un$.

Next, assuming $\|\theta\|$ is small, we suppose that $S_\theta^2 \approx 0$, $C_\theta^2 \approx 1$, $\sin\theta_i \approx \theta_i$, and we find that $Ke = 0, De = 0$. Therefore, some of the components of the equation can be approximated as

$$[lS_\theta K, -lC_\theta K]\begin{bmatrix} m + u_n S_\theta^2 & -u_n S_\theta C_\theta \\ -u_n S_\theta C_\theta & m + u_n C_\theta^2 \end{bmatrix}\begin{bmatrix} \ddot{X} \\ \ddot{Y} \end{bmatrix} = (m + u_n)l^2KK^{\mathrm{T}}\ddot{\theta} + u_n lKS_\theta e\ddot{p_x},$$

$$[lS_\theta K, -lC_\theta K]\begin{bmatrix} c_t C_\theta^2 + c_n \times S_\theta^2 & (c_t - c_n)S_\theta C_\theta \\ (c_t - c_n)S_\theta C_\theta & c_t S_\theta^2 + c_n \times C_\theta^2 \end{bmatrix}\begin{bmatrix} \dot{X} \\ \dot{Y} \end{bmatrix} = (c_t + c_n)l^2KK^{\mathrm{T}}\dot{\theta} + (c_n - c_t)\dot{p_x}l\theta K,$$

$$\zeta_1(t) = [lS_\theta K, -lC_\theta K]\begin{bmatrix} c_t C_\theta & -c_n S_\theta \\ c_t S_\theta & c_n C_\theta \end{bmatrix}\begin{bmatrix} v_{rx}^2 \\ v_{ry}^2 \end{bmatrix} \times \operatorname{sign}\left(\begin{bmatrix} v_{rx} \\ v_{ry} \end{bmatrix}\right).$$

Among those equations, omitted items as disturbances. For control design purposes, we model the hydrodynamic phenomena in the form of analytical expression and meanwhile taking into account significant hydrodynamic effects, and let remainder function $\zeta_1(t)$ as unmodeled dynamics item. We get the approximate equations of motion of the first row

$$J\ddot{\theta} + \mu J\theta + M_v\theta + \sigma_1 = D^{\mathrm{T}}u,$$

where

$$J = (m + u_n)l^2(\frac{1}{3}I_n + KK^{\mathrm{T}}), \quad \mu = \frac{(c_t + c_n)}{m + u_n}, \quad M_v = (c_n - c_t)\dot{p}_x lK,$$

$$\sigma_1 = \zeta_1(t) + \frac{1}{3}l^2(c_n - c_t)\dot{\theta} + u_n\ddot{p}_x lK\theta + \frac{1}{2}l^4\dot{\theta}.$$

Then, we continue simplification and define the joint angle $\phi \in \mathbb{R}^{n-1}$, orientation angle $\varphi \in \mathbb{R}$ as follows: $\begin{bmatrix} \phi \\ \varphi \end{bmatrix} = \begin{bmatrix} D \\ \frac{e^{\mathrm{T}}}{(n-1)} \end{bmatrix}\theta$, $[T, e] := W = \begin{bmatrix} D \\ \frac{e^{\mathrm{T}}}{(n-1)} \end{bmatrix}^{-1}$. Multiply by W^{T} from the left and let $W^{\mathrm{T}}JW = \begin{bmatrix} J_{11} & J_{12} \\ J_{11} & J_{22} \end{bmatrix}$. Consider the matrix $U := \begin{bmatrix} I & -J_{12}^{-1}J_{22} \\ -J_{21}^{-1}J_{11} & 1 \end{bmatrix}$. Multiply by U from the left. This item reduced to $UW^{\mathrm{T}}JW = \begin{bmatrix} J_1 & 0 \\ 0 & J_2 \end{bmatrix}$, where J_1, J_2 is the remainder. The above motion equation is reduced to

$$\ddot{\phi} + \mu\dot{\phi} + M_{v1}\phi + J_1^{-1}\sigma_{\phi 1} = J_1^{-1}u. \tag{A1}$$

The orientation joint dynamics is reduced to

$$\ddot{\varphi} + \mu\dot{\varphi} + M_{v2}\phi + J_2^{-1}\sigma_{\varphi 1} = -J_2^{-1}J_{21} \times J_{11}^{-1}u, \tag{A2}$$

where remainder $\begin{bmatrix} \sigma_{\phi 1} \\ \sigma_{\varphi 1} \end{bmatrix} := UW^{\mathrm{T}}\sigma_1(t)$ is the corresponding force unmodeled dynamics item. Corresponding coefficients are defined by

$$M_{v1} = \dot{p}_x(c_n - c_t)J_1^{-1}(T^{\mathrm{T}}T - J_{12}J_{22}^{-1}e^{\mathrm{T}}KT), \quad M_{v2} = \dot{p}_x(c_n - c_t)J_2^{-1}(e^{\mathrm{T}}KT - J_{21}J_{11}^{-1}T^{\mathrm{T}}KT).$$

Note that $\theta = T\phi + e\varphi$,$e^{\mathrm{T}}T = 0, DT = I_{n-1}$. To this end, we choose an reference velocity in x-direction $\dot{p}_x = \dot{p}_{x0}$. we get this form:

$$\ddot{\phi} + \mu\dot{\phi} + M_{v1}(\dot{p}_{x0})\phi + \sigma_\phi = J_1^{-1}u, \quad \ddot{\varphi} + \mu\dot{\varphi} + M_{v2}(\dot{p}_{x0})\phi + \sigma_\varphi = -J_2^{-1}J_{21} \times J_{11}^{-1}u,$$

where remainder is defined as $\sigma_\phi = M_{v1}\phi - M_{v1}(\dot{p}_{x0})\phi + J_1^{-1}\sigma_{\phi 1}$,and $\sigma_\varphi = M_{v2}\phi - M_{v2}(\dot{p}_{x0})\phi + +J_2^{-1}\sigma_{\varphi 1}$ is defined as unmodeled dynamics, where $\begin{bmatrix}\sigma_{\phi 1}\\ \sigma_{\varphi 1}\end{bmatrix}$ is completely eliminated by control input $u(t)$. We will have

$$\ddot{\phi} + \mu\dot{\phi} + M_{v1}(\dot{p}_{x0})\phi = J_1^{-1}u_{\mathrm{ref}}, \quad \ddot{\varphi} + \mu\dot{\varphi} + M_{v2}(\dot{p}_{x0})\phi = -J_2^{-1}J_{21} \times J_{11}^{-1}u_{\mathrm{ref}}.$$

The force balance equation keep the nonlinear equation form and will be used in orientation controller simulation to declare the effectiveness of the modified adaptive controller.

Other coefficients are defined by $\begin{bmatrix}v_{rx}\\ v_{ry}\end{bmatrix} = \begin{bmatrix}C_\theta & S_\theta\\ -S_\theta & C_\theta\end{bmatrix}\begin{bmatrix}\dot{X}\\ \dot{Y}\end{bmatrix}$, $A := [I_{n-1}, 0_{n-1}] + [0_{n-1}, I_{n-1}]$, $D := [I_{n-1}, 0_{n-1}] - [0_{n-1}, I_{n-1}]$, $e := [1 \dots 1]^{\mathrm{T}}$, $\cos\theta := [\cos\theta_1, \dots, \cos\theta_n]^{\mathrm{T}}$, $\sin\theta := [\sin\theta_1, \dots, \sin\theta_n]^{\mathrm{T}}$, $K := A^{\mathrm{T}}(DD^{\mathrm{T}})^{-1}D$, $S_\theta := \mathrm{diag}(\sin\theta)$, $C_\theta := \mathrm{diag}(\cos\theta)$, $E := \begin{bmatrix}e & 0_{n\times 1}\\ 0_{n\times 1} & e\end{bmatrix}$, and subscript $n-1$ stands for $n-1$ dimensions.

Generally speaking, the full nonlinear dynamics equations are reduced to approximate dynamics equations by supposing $\begin{bmatrix}\phi\\ \varphi\end{bmatrix}$ is small. If φ is not small, we can use a new variable $\varphi_{\mathrm{new}} := \varphi - \varphi_0$, which means a new global coordinates of the center of mass of the snake-like robot. φ_0 is a constant value. Anyways, only if the amplitudes of ϕ and φ are small enough, the full nonlinear dynamics equations can be reduced to approximate dynamics equations.